Nanosecond pulsed electric fields perturb membrane phospholipids in T lymphoblasts☆

P. Thomas Vernier[a,b,*], Yinghua Sun[c], Laura Marcu[a,d,e], Cheryl M. Craft[f], Martin A. Gundersen[a]

[a] *Department of Electrical Engineering-Electrophysics, School of Engineering, University of Southern California, Los Angeles, CA 90089-0271, USA*
[b] *MOSIS, Information Sciences Institute, School of Engineering, University of Southern California, Los Angeles, CA 90292-6695, USA*
[c] *Department of Materials Science, School of Engineering, University of Southern California, Los Angeles, CA 90089-0271, USA*
[d] *Department of Biomedical Engineering, School of Engineering, University of Southern California, Los Angeles, CA 90089-0271, USA*
[e] *Biophotonics Research and Technology Development Laboratory, Department of Surgery, Cedars-Sinai Medical Center, Los Angeles, CA 90048, USA*
[f] *Mary D. Allen Laboratory for Vision Research, Doheny Eye Institute, and Department of Cell and Neurobiology, Keck School of Medicine, University of Southern California, Los Angeles, CA 90089-9112, USA*

Received 9 April 2004; revised 2 July 2004; accepted 3 July 2004

Available online 22 July 2004

Edited by Gerrit van Meer

Abstract Nanosecond, megavolt-per-meter pulsed electric fields scramble the asymmetric arrangement of phospholipids in cell membranes without the permeabilization associated with longer, lower-field pulses. A single 30 ns, 2.5 MV/m pulse produces perturbations consistent with phosphatidylserine (PS) externalization in Jurkat T lymphoblasts within milliseconds, polarized in the direction of the applied field, indicating an immediate interaction between membrane components and the electric field. This disturbance occurs only at the anode pole of the cell, supporting the hypothesis that the pulsed field drives the negatively charged PS head group toward the positive electrode, directly providing the energy for crossing the membrane dielectric barrier.

Keywords: Nanosecond pulsed electric field; Phosphatidylserine externalization; Phospholipid translocation; Real-time fluorescence microscopy

1. Introduction

Recent studies have confirmed theoretical predictions that ultra-short, high-field electric pulses can induce intracellular responses (eosinophil sparklers [1], calcium bursts [2], and apoptosis [3,4]) in the absence of membrane permeabilization and other effects associated with electroporation. Although nanoelectropulsed cells are not porated by conventional measure, membrane phospholipid scrambling is consistently observed, indicating that nanosecond pulsed electric fields can modify the organization of the plasma membrane. Some cell types recover from the disturbance [3]. In others the distress display of phosphatidylserine (PS) on the external face of the cell persists and additional signs of nanoelectropulse-induced apoptosis appear [5]. PS externalization – the translocation of PS from its normal position on the cytoplasmic face of the plasma membrane to the exterior of the cell – has been extensively studied, as a diagnostic sign of apoptosis [6,7] and as a component of other physiological processes associated with cell senescence and phagocytic removal [8]. The ability to activate this signal remotely, with non-ionizing, non-thermal (high power, but low total energy), non-invasive electric pulses may be useful in both research and clinical settings.

Because PS translocation is an early event in nanoelectropulse-induced apoptosis [9], and because considerable progress has been made toward characterization of the biophysics and physiology of this phenomenon [10], an investigation of pulse-induced PS externalization should illuminate proposed mechanisms for PS transbilayer migration and provide at the same time information about the responses of cells to nanosecond pulsed electric fields. Our observations support the hypothesis that PS translocation is immediately associated with the application of the pulse and that it is a field-driven event, with no more than a few milliseconds intervening between the arrival of the pulse edge and the appearance of PS molecules on the external face of the cell.

2. Materials and methods

2.1. Cell lines and culture conditions

Human Jurkat T lymphocytes (ATCC TIB-152) were grown in RPMI 1640 (Irvine Scientific, Irvine, CA) containing 10% heat-inactivated fetal bovine serum (FBS; Gibco, Carlsbad, CA), 2 mM L-glutamine (Gibco), 50 units/mL penicillin (Gibco), and 50 μg/mL streptomycin (Gibco) at 37 °C in a humidified, 5% carbon dioxide atmosphere.

2.2. Pulse generator and pulse exposures

For microscopic observations, cells were placed in a rectangular channel 100 μm wide, 30 μm deep, and 12 mm long, with gold-plated electrode walls, microfabricated with photolithographic methods on a glass microscope slide. A fast MOSFET MicroPulser [11] was mounted on the microscope stage for delivery of pulses directly to the microchamber electrodes in ambient atmosphere at room temperature.

☆ Supplementary data associated with this article can be found, in the online version, at doi:10.1016/j.febslet.2004.07.021.

* Corresponding author. Fax: +1-310-823-5624.
E-mail addresses: vernier@mosis.org (P.T. Vernier), yinghuas@usc.edu (Y. Sun), lmarcu@bmsrs.usc.edu (L. Marcu), ccraft@usc.edu (C.M. Craft), mag@usc.edu (M.A. Gundersen).

Abbreviations: BAPTA, 1,2-bis(*o*-aminophenoxy)ethane-*N*,*N*,*N*′,*N*′-tetraacetic acid; FM1-43, *N*-(3-triethylammoniumpropyl)-4-(4-(dibutylamino)styryl)pyridinium dibromide; PS, phosphatidylserine

0014-5793/$22.00
doi:10.1016/j.febslet.2004.07.021

2.3. Fluorescence microscopy

Observations of live cells during pulse exposures were made with a Zeiss Axiovert 200 epifluorescence microscope. For visualization of PS translocation with FM1-43 (Molecular Probes; $\lambda_{ex} = 480$ nm, $\lambda_{em} = 535$ nm), cells were washed twice, resuspended in growth medium containing 20 μM FM1-43, incubated for 20 min at 37 °C, and observed without additional washing. EGTA was from Calbiochem, cytochalasin D from Sigma–Aldrich, and thapsigargin and BAPTA-AM from Molecular Probes. Images were captured and analyzed with a LaVision PicoStar HR12 camera and software (LaVision, Goettingen, Germany). Photometric data are from at least 20 representative cells from three independent experiments. Error bars represent the standard error of the sample mean.

3. Results

Membrane phospholipid asymmetry is maintained by appropriately balanced aminophospholipid translocase [12] and scramblase [13] activities, in concert with membrane synthesis and recycling [14]. To determine whether nanoelectropulse-induced PS translocation is realized through a shift in this equilibrium (in which case the externalization would be expected to occur some time after pulse exposure – perhaps many seconds or even minutes), or whether it is a result of a direct field effect on the membrane (which should be immediately observable at pulse time), a fast-responding measure of PS externalization is required – ideally on the nanosecond time scale of the pulses.

PS externalization is conventionally detected with annexin V, a protein that binds specifically to sections of the cell membrane containing exposed PS head groups [15], but this assay is unsuitable for real-time observations of rapid events. The binding kinetics are too slow at standard reactant concentrations, and background fluorescence from unbound, fluorochrome-tagged annexin V necessitates washing the cells after incubation, a step that is incompatible with continuous monitoring of suspended cells by microscopic or other means.

N-(3-triethylammoniumpropyl)-4-(4-(dibutylamino)styryl) pyridinium dibromide (FM1-43), a cationic styryl fluorochrome that partitions between the aqueous medium and the cytoplasmic membrane, has been identified as an effective and rapidly responsive indicator of PS translocation in Jurkat cells [16]. Although FM1-43 is soluble in aqueous media, insertion of its hydrocarbon tail into lipid membranes is thermodynamically favored [17], and the quaternary ammonium in the head group prevents migration across the lipid bilayer. Translocation of the negatively charged PS head group to the outer face of the membrane provides additional electrostatic attraction for the quaternary ammonium of FM1-43, resulting in more dye binding per unit area and a concomitant increase in fluorescence emission. The fluorescence quantum yield of FM1-43 increases by several orders of magnitude on membrane binding [17], enabling real-time microscopic observations of changes in externalized PS by eliminating the need for washing.

FM1-43 uniformly stains the cytoplasmic membrane of resting Jurkat cells, which show little fluorescence in the cell interior [18]. In our experiments with actively growing cells, membrane material is continuously cycling into intracellular vesicles, carrying the FM1-43 with it, so that we observe the plasma membrane as a clearly demarcated line of fluorescence at the perimeter of the cell, and in addition a heterogeneous distribution of intracellular membrane-bound structures (Fig. 1). Because the increased FM1-43 fluorescence associated with PS externalization results from the insertion of additional dye molecules into the membrane, the time resolution for observations of PS translocation is limited by the rate of diffusion of FM1-43 to the medium-membrane interface and by the rate of insertion of the FM1-43 tail into the array of phospholipids

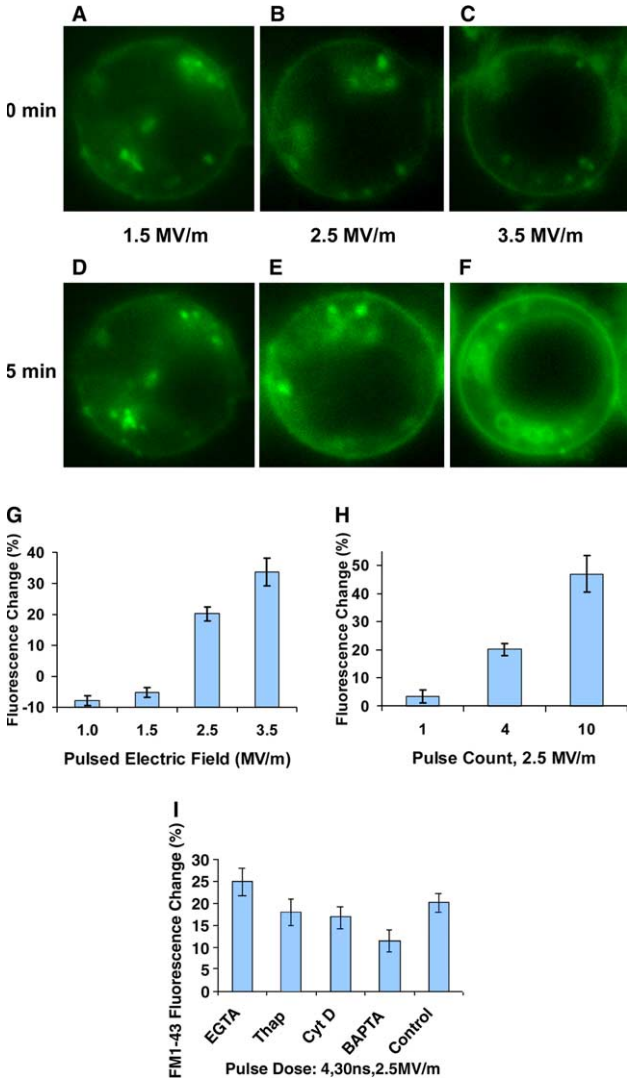

Fig. 1. PS externalization response with increasing pulsed field strength and pulse count and after disruption of Ca^{2+} distribution and actin polymerization. Representative Jurkat cells stained with FM1-43 are shown before (A–C) and 5 min after (D–F) exposure to 4, 30 ns pulses at 1.5, 2.5, and 3.5 MV/m. Increased FM1-43 fluorescence indicates translocation of PS to the external face of the cytoplasmic membrane. (G) Integrated, whole-cell, FM1-43 fluorescence changes 5 min after exposure to 4, 30 ns pulses of 1.0, 1.5, 2.5, and 3.5 MV/m. (H) Integrated, whole-cell, FM1-43 fluorescence changes 5 min after exposure to 1, 4, and 10, 30 ns pulses of 2.5 MV/m delivered to separate groups of cells with a pulse repetition rate of 4 Hz. Data are from at least 20 representative cells from three independent experiments. (I) Integrated, whole-cell, FM1-43 fluorescence changes 5 min after exposure to 4, 30 ns, 2.5 MV/m pulses. Cells were incubated in the presence of 5 mM EGTA for 15 min, 1 μM thapsigargin and 10 μM cytochalasin D for 30 min, and 10 μM BAPTA-AM for 60 min at 37 °C before pulse exposure. Data are from at least 20 representative cells from three independent experiments. Error bars show the standard error of the sample mean.

at the membrane surface. At room temperature with 4 μM FM1-43, we detect pulse-induced changes photometrically within 400 ms. Equilibration after a pulsed electric field exposure is complete within 5 min.

Nanoelectropulse-induced FM1-43 fluorescence increases with both pulse amplitude and pulse count. Fig. 1A–F shows the response of typical FM1-43-stained Jurkat cells before and 5 min after exposure to 4, 30 ns pulses with field strengths ranging from 1.5 to 3.5 MV/m. No fluorescence increase is observed with fields up to 1.5 MV/m, consistent with previous observations [3], and 3.5 MV/m pulses elicit a stronger response than 2.5 MV/m (Fig. 1G). Morphological changes are evident in cells pulsed at 3.5 MV/m, a dose near the increased lethality limit reported for 7 and 20 ns pulses delivered to Jurkat cells [3]. Fig. 1H summarizes the response to multiple 30 ns, 2.5 MV/m pulses – 1, 4, and 10 pulses delivered to separate groups of cells at 0.25 ms intervals. The single-pulse change is near the sensitivity of the imaging system; 4 and 10 pulses produce, respectively, greater fluorescence intensification.

These results are consistent with our earlier reports of a minimum field required for nanoelectropulse-induced PS externalization (annexin V binding) [3,9]. On the basis of these data, we conclude that for pulse durations from 7 to 30 ns in growth medium at 25 °C, the field strength threshold for membrane phospholipid rearrangement resulting in PS externalization in actively metabolizing Jurkat cells lies between 1.0 and 2.5 MV/m. Furthermore, microscopic observations of individual cells make it clear that the increased amount of PS translocation observed after multiple pulses is not a population phenomenon, where one sub-population of cells is more sensitive than another, but rather a multiple-dose effect at the single-cell level. Although some cells are more responsive than others in absolute terms, each responding cell fluoresces more intensely with increasing pulse dosage.

Since the enzymes that regulate PS asymmetry are sensitive to calcium [13,19], and since we have demonstrated previously the nanoelectropulse induction of intracellular calcium bursts [2], we carried out the experiments summarized in Fig. 1I to determine whether nanoelectropulse-induced PS translocation is caused by elevated, post-pulse intracellular calcium levels. Our previous work has shown that adding the calcium chelating agent EGTA to the external medium has no effect on the appearance of intracellular calcium bursts in cells exposed to ultra-short pulsed electric fields. We report now that EGTA does not inhibit the post-pulse intensification of membrane-bound FM1-43 fluorescence (Fig. 1I). The calcium chelator BAPTA, introduced into the cell as the acetoxymethyl ester, slightly depresses pulse-induced FM1-43 fluorescence intensification (P value from Student's unpaired t test <0.01). Neither the endoplasmic reticulum ATPase calcium pump inhibitor thapsigargin [20] nor the cytoskeletal actin polymerization inhibitor cytochalasin D [19], which depress nanoelectropulse-induced calcium bursts [2, unpublished observations], has a significant effect (P value >0.10). From these results, we conclude that while intracellular chelation of calcium measurably affects pulse-induced PS externalization, no clear and requisite role for calcium is apparent.

If calcium-stimulated, enzyme-mediated transbilayer migration of PS is not the mechanism for nanoelectropulse-driven PS externalization, what alternative, "calcium-free" hypotheses might be considered? We suggest two – nanopore-facilitated diffusion and direct field-induced transport – and we provide evidence that argues against the former and in favor of the latter.

Although we have shown elsewhere that nanoelectropulses with the durations and field strengths used in these experiments do not cause detectable cation influx from the medium into Jurkat cells [2], we cannot exclude the possibility that nanosecond-duration, nanometer-diameter pores are formed under these conditions [9], providing a lower-energy translocation path from the inner to the outer membrane surface (Fig. 2A). The two faces of the membrane form a continuum at the periphery of such a pore, modifying the hydrophobic barrier to transmembrane movement of the charged phospholipid head groups [21], and permitting PS molecules to migrate, perhaps in a process related to "lateral" diffusion [22], from the interior to the exterior face of the cell at micrometer-per-second rates [23].

To detect membrane nanoporation, we loaded cells with the calcium-sensitive dye Calcium Green [2], applied pulses with manganese in the medium, and looked for fluorescence quenching by Mn^{2+} ions [24], which are excluded from the cytoplasm in the short term by an intact membrane. The results confirm our previous observations. Long, microsecond pulses porate the membrane, resulting in Mn^{2+} entry and quenching of Calcium Green fluorescence (Fig. 3A). Mn^{2+} influx is not detected with nanosecond pulse exposures (Fig. 3B).

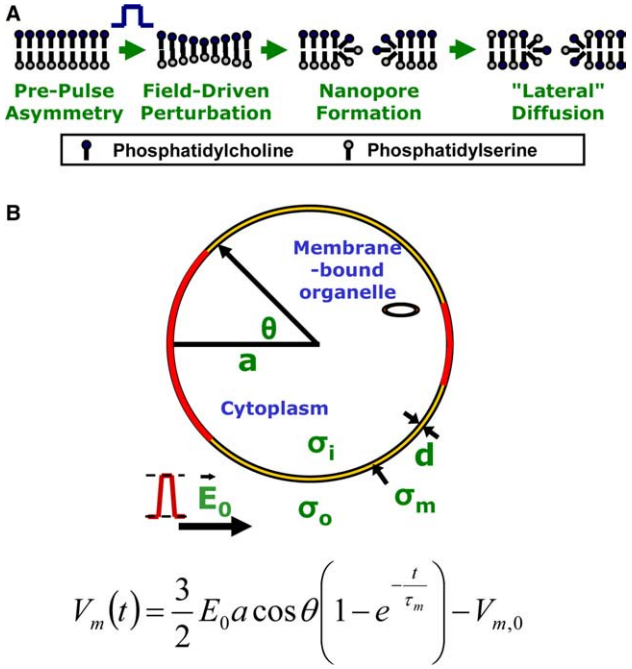

$$V_m(t) = \frac{3}{2} E_0 a \cos\theta \left(1 - e^{-\frac{t}{\tau_m}}\right) - V_{m,0}$$

Fig. 2. Nanopore-facilitated phospholipid translocation and porated dielectric shell model. (A) Model for PS externalization at the perimeter of transient, nanometer-diameter pores formed in response to nanoelectropulse perturbation of the membrane. (B) Dielectric shell model of a biological cell in a pulsed electric field, showing regions of greater transmembrane voltage (V_m) at the anode (left) and cathode (right) poles of the cell, reflected in the cosine term in the simplified time-dependent solution to Laplace's equation for this system, where E_0 is the applied electric field, a is the cell radius, θ is the position angle relative to the electric field, t is the time after the initiation of the pulse, and τ_m is the membrane charging time constant.

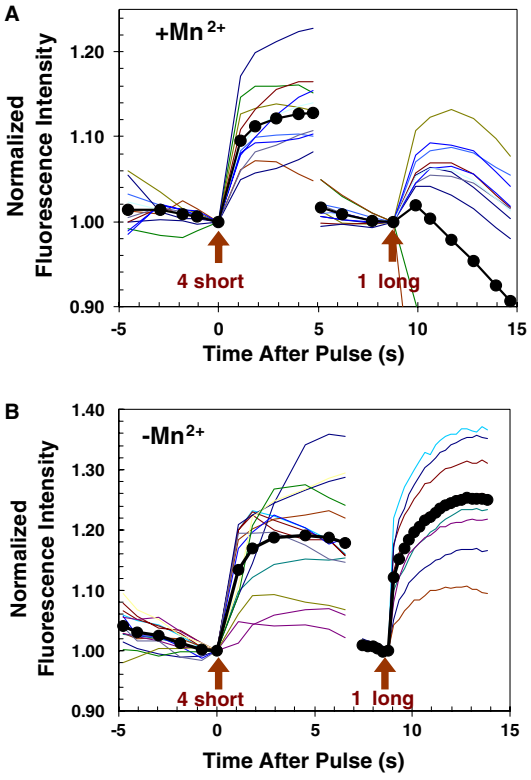

Fig. 3. Mn^{2+} exclusion from nanoelectropulsed cells. Four ultra-short pulses (30 ns, 2.5 MV/m) produce a calcium burst (increase in intracellular Calcium Green fluorescence) with (A) or without (B) 250 μM Mn^{2+} in the external medium. A single long pulse (10 μs, 0.5 MV/m), causes Mn^{2+} influx and fluorescence quenching (A). Circles are average integrated fluorescence intensity values. Light lines are individual cell responses.

If nanoelectropulse-induced PS translocation results from facilitated diffusion at porated "bridges" across the lipid bilayer energy barrier, then the dielectric shell model of the cell [25] and previous observations of electroporated cells [26,27] predict that PS externalization will be observed at both the anode and the cathode poles of the cell (Fig. 2B). We tested this model using FM1-43 fluorescence as an indicator of PS translocation.

Microscopic observations of FM1-43-stained Jurkat cells during pulse exposure reveal a transient anodic fluorescence intensification consistent with PS externalization (Fig. 4). A cap of increased fluorescence emission appears at the anode pole of nanoelectropulsed cells within 400 ms of the application of the pulse. (Time resolution is limited by the sensitivity of our imaging system.) No intensification is observed initially at other locations, including at the cathode pole. Then, over a period of about one minute, the fluorescence emission around the entire circumference of the cell increases until the pattern is uniform. This represents two post-pulse processes. First, the membrane constituents localized at the pulse-induced regions of increased FM1-43 fluorescence (which we interpret to be an

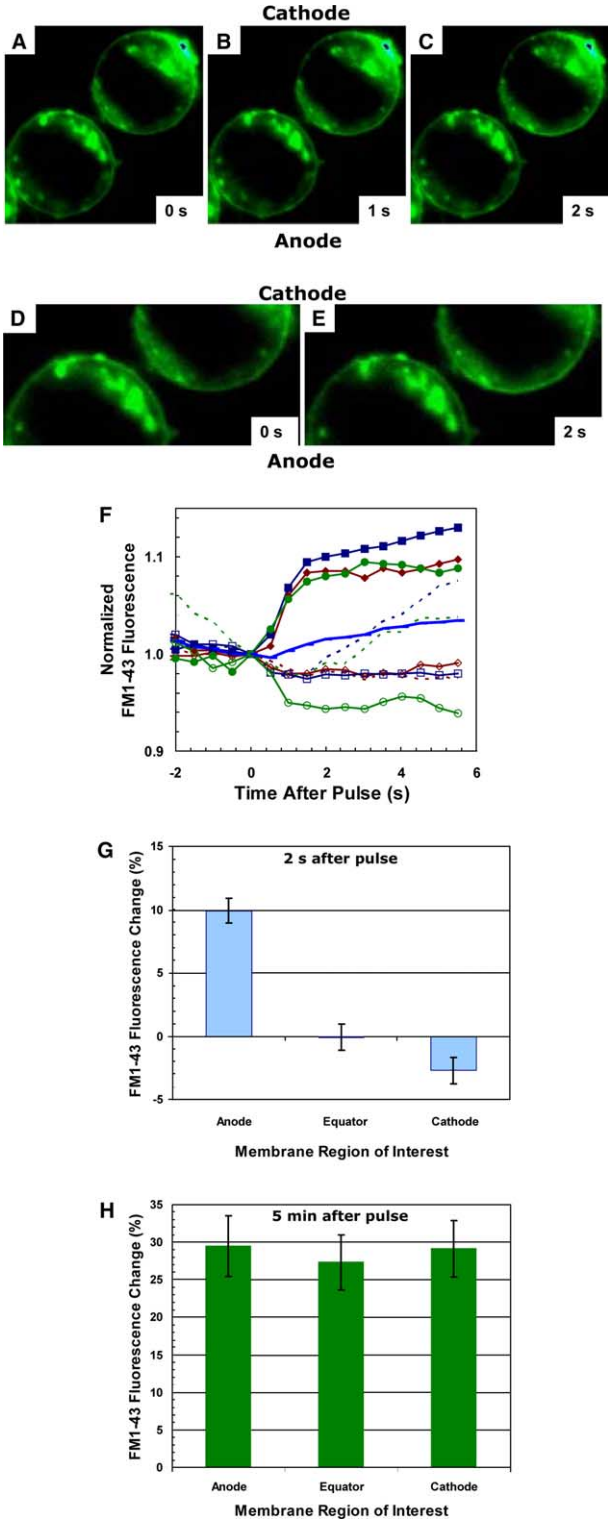

Fig. 4. Nanoelectropulse-driven PS externalization restricted to the anode pole. Immediate post-pulse FM1-43 fluorescence intensification is restricted to the cytoplasmic membrane at the anode pole (bottom of image) of Jurkat cells (A–C; enlarged images in D,E). Anode-localized, PS translocation indicated by increased FM1-43 fluorescence occurs in less than 1 s (B,F). Solid symbols in (F) are from the anode pole; open symbols are from the cathode pole. Dissipation of translocated PS polar cap by lateral diffusion (G,H). The anodic concentration of nanoelectropulse-translocated PS (G) becomes a homogeneous distribution within 5 min (H) as the externalized PS diffuses laterally in the outer leaflet of the membrane bilayer. Fluorescence intensity is taken from anode, equator, and cathode regions of interest 2.4 μm × 0.5 μm (22 pixels × 5 pixels). Cell diameters are approximately 10 μm. (The anode pole of the cell is nearer to the positive electrode; the cathode pole is closer to the negative electrode.) Data are from at least 20 representative cells from three independent experiments. Error bars show the standard error of the sample mean.

indication of translocated PS) at the anode end of the cell rapidly diffuse circumferentially throughout the outer monolayer of the plasma membrane. Second, in response to the overall higher concentration of PS now exposed on the external face of the cell, FM1-43 diffuses from the medium into the membrane, producing a net increase of fluorescence emission uniformly distributed over the surface of the cell (Fig. 4H). Localized FM1-43 fluorescence intensification after nanoelectropulse exposure is never seen in FM1-43-stained intracellular vesicles, consistent with the assumption that the observed fluorescence increase does not arise from dye molecules in the cell membranes at pulse time but rather from additional FM1-43 that enters the cytoplasmic membrane from the medium in response to the pulse-induced increase in PS molecules available at the exposed face of the cell.

The absence of both Mn^{2+} influx and cathodic FM1-43 fluorescence brightening, combined with previously reported evidence against poration by ultra-short pulsed electric fields, calls into question the hypothesis that nanosecond pulse-induced PS externalization results from facilitated phospholipid lateral diffusion at transient membrane nanopores.

4. Discussion

The appearance of nanoelectropulse-translocated PS only at the anode pole of the cell is consistent with direct, electric field-driven transport of the anionic PS head group across the Born energy barrier of the lipid interior of the membrane, on the order of 100 kJ/mol for a homogeneous phospholipid bilayer [28]. For the pulse conditions reported here, the transmembrane potential calculated from the simple dielectric shell model of the cell (Fig. 2B) reaches 1 V, already sufficient to provide the necessary translocation activation energy (1 eV $\cong$ 100 kJ/mol). Pulse-associated perturbations acting on critical features of cell membrane architecture may lower this activation energy and facilitate translocation and the requisite accompanying membrane restructuring in less direct ways, including thermal- and electric field-induced lipid phase transitions, lipid raft redistribution and the dynamic reorganization of cytoskeletal-membrane attachments, dipole effects on membrane-spanning peptides, the nanoscale release of Ca^{2+} from internal stores, and the proximity of nanoelectropulse-depolarized mitochondria [29].

The fact that FM1-43 fluorescence intensification is restricted to the anode-proximate region of the membrane does not rule out the possibility of nanoporation at one or both poles. Observers monitoring long (microsecond)-pulse electroporation report differences in conductance and permeability [26,27] at the anode and cathode ends of cells that may reflect structural asymmetries between inwardly and outwardly hyperpolarized membranes, and these may affect the phospholipid translocation mechanism. On the other hand, the small but significant *decrease* in FM1-43 fluorescence observed at the cathode pole (Fig. 4G) may indicate the field-driven, inward (toward the anode) translocation of negatively charged phospholipids or other ionic species, consistent with the direct field-driven translation hypothesis.

One test of these alternate mechanisms calls for shorter pulses with correspondingly higher fields. If PS externalization is a consequence of the electrostatic potential developed across the cytoplasmic membrane during a 7–30 ns, 2.5 MV/m pulse [9], then a pulse which is too short to charge the membrane to the conductive breakdown potential [30], and which therefore produces less than the 10–20 MV/m field (0.5–1 eV) in the membrane dielectric generated in the experiments described here, should not cause immediate PS translocation (but may have other effects, consequences of the high field delivered to the intracellular environment). The direct field-driven translation hypothesis predicts also that a phospholipid with a positively charged head group will be externalized at the cathode end of the cell, and not at the anode, and that a series of pulses, alternating in polarity, will translocate phospholipids at both poles of the cell. Investigations of the mechanisms for immediate nanoelectropulse-induced PS externalization must take into account the possibility that other processes associated with cellular stress responses, including apoptosis, may contribute overlapping and complicating symptoms, and that PS exposure after nanoelectropulse treatment may itself be a two-stage process [1,3,31].

Exploration of these possibilities promises to uncover not only basic cell biology and bioelectrics information but also pathways to practical applications. The ability to flip the membrane phospholipid switch with remotely delivered nanosecond electric pulses suggests the development of pulse exposure recipes (with pulse trains of varying amplitude, duration, and pattern) for selectively triggering responses in different cell types [1,3] depending on their dielectric properties [32], leading to the elimination of undesirable cell populations by inducing them to advertise for phagocytic engulfment or to initiate directly their own apoptotic demise.

Acknowledgements: We thank Matthew Behrend for pulse generator design and assembly, Mya Thu, Katherine Chiu, and Jingjing Wang for cell culture and technical expertise, and Sarah Salemi for fluorescence microscopy. This work was made possible by support from the Air Force Office of Scientific Research and the Army Research Office, and by NIH grant EY00395 (C.M.C.). C.M.C. is the Mary D. Allen Chair in Vision Research, Doheny Eye Institute, University of Southern California.

References

[1] Schoenbach, K.H., Beebe, S.J. and Buescher, E.S. (2001) Bioelectromagnetics 22, 440–448.
[2] Vernier, P.T., Sun, Y., Marcu, L., Salemi, S., Craft, C.M. and Gundersen, M.A. (2003) Biochem. Biophys. Res. Commun. 310, 286–295.
[3] Vernier, P.T., Li, A., Marcu, L., Craft, C.M. and Gundersen, M.A. (2003) IEEE Trans. Dielectr. Electr. Insul. 10, 795–809.
[4] Beebe, S.J., Fox, P.M., Rec, L.J., Somers, K., Stark, R.H. and Schoenbach, K.H. (2002) IEEE Trans. Plasma Sci. 30, 286–292.
[5] Beebe, S.J., Fox, P.M., Rec, L.J., Willis, E.L. and Schoenbach, K.H. (2003) FASEB J. 17, 1493–1495.
[6] Martin, S.J., Reutelingsperger, C.P., McGahon, A.J., Rader, J.A., van Schie, R.C., La Face, D.M. and Green, D.R. (1995) J. Exp. Med. 182, 1545–1556.
[7] Tanaka, Y. and Schroit, A.J. (1983) J. Biol. Chem. 258, 11335–11343.
[8] Zhang, G., Gurtu, V., Kain, S.R. and Yan, G. (1997) Biotechniques 23, 525–531.
[9] Vernier, P.T., Sun, Y., Marcu, L., Craft, C.M. and Gundersen, M.A. (2004) Biophys. J. 86, 4040–4048.
[10] Fadok, V.A., de Cathelineau, A., Daleke, D.L., Henson, P.M. and Bratton, D.L. (2001) J. Biol. Chem. 276, 1071–1077.
[11] Behrend, M., Kuthi, A., Gu, X., Vernier, P.T., Marcu, L., Craft, C.M. and Gundersen, M.A. (2003) IEEE Trans. Dielectr. Electr. Insul. 10, 820–825.

[12] Seigneuret, M. and Devaux, P.F. (1984) Proc. Natl. Acad. Sci. USA 81, 3751–3755.
[13] Basse, F., Stout, J.G., Sims, P.J. and Wiedmer, T. (1996) J. Biol. Chem. 271, 17205–17210.
[14] Bevers, E.M., Comfurius, P., Dekkers, D.W. and Zwaal, R.F. (1999) Biochim. Biophys. Acta 1439, 317–330.
[15] Koopman, G., Reutelingsperger, C.P., Kuijten, G.A., Keehnen, R.M., Pals, S.T. and van Oers, M.H. (1994) Blood 84, 1415–1420.
[16] Zweifach, A. (2000) Biochem. J. 349, 255–260.
[17] Schote, U. and Seelig, J. (1998) Biochim. Biophys. Acta 1415, 135–146.
[18] Wurth, G.A. and Zweifach, A. (2002) Biochem. J. 362, 701–708.
[19] Kunzelmann-Marche, C., Freyssinet, J.-M. and Martinez, M.C. (2001) J. Biol. Chem. 276, 5134–5139.
[20] Thastrup, O., Cullen, P.J., Drobak, B.K., Hanley, M.R. and Dawson, A.P. (1990) Proc. Natl. Acad. Sci. USA 87, 2466–2470.
[21] Homan, R. and Pownall, H.J. (1988) Biochim. Biophys. Acta 938, 155–166.
[22] Sonnleitner, A., Schutz, G.J. and Schmidt, T. (1999) Biophys. J. 77, 2638–2642.
[23] Fujiwara, T., Ritchie, K., Murakoshi, H., Jacobson, K. and Kusumi, A. (2002) J. Cell Biol. 157, 1071–1081.
[24] Hallam, T.J. and Rink, T.J. (1985) FEBS Lett. 186, 175–179.
[25] Plonsey, R. and Altman, K.W. (1998) Proc. IEEE 76, 1122–1129.
[26] Hibino, M., Shigemori, M., Itoh, H., Nagayama, K. and Kinosita, K. (1991) Biophys. J. 59, 209–220.
[27] Gabriel, B. and Teissie, J. (1999) Biophys. J. 76, 2158–2165.
[28] Parsegian, A. (1969) Nature 221, 844–846.
[29] Blom, W.M., De Bont, H.J. and Nagelkerke, J.F. (2003) J. Biol. Chem. 278, 12467–12474.
[30] Zimmermann, U. (1982) Biochim. Biophys. Acta 694, 227–277.
[31] Hammill, A.K., Uhr, J.W. and Scheuermann, R.H. (1999) Exp. Cell Res. 251, 16–21.
[32] Polevaya, Y., Ermolina, I., Schlesinger, M., Ginzburg, B.-Z. and Feldman, Y. (1999) Biochim. Biophys. Acta 1419, 257–271.